



This is a repository copy of *Annealing impact on mechanical performance and failure analysis assisted with acoustic inspection of carbon fiber reinforced poly-ether-ketone-ketone composites under flexural and compressive loads*.

White Rose Research Online URL for this paper:

<https://eprints.whiterose.ac.uk/219217/>

Version: Published Version

Article:

Elmas, S. orcid.org/0000-0002-9745-9680, Atac, B., Senol, C.O. et al. (3 more authors) (2025) Annealing impact on mechanical performance and failure analysis assisted with acoustic inspection of carbon fiber reinforced poly-ether-ketone-ketone composites under flexural and compressive loads. *Polymer Composites*, 46 (4). pp. 3686-3704. ISSN 0272-8397

<https://doi.org/10.1002/pc.29199>

Reuse

This article is distributed under the terms of the Creative Commons Attribution-NonCommercial-NoDerivs (CC BY-NC-ND) licence. This licence only allows you to download this work and share it with others as long as you credit the authors, but you can't change the article in any way or use it commercially. More information and the full terms of the licence here: <https://creativecommons.org/licenses/>

Takedown

If you consider content in White Rose Research Online to be in breach of UK law, please notify us by emailing eprints@whiterose.ac.uk including the URL of the record and the reason for the withdrawal request.



eprints@whiterose.ac.uk
<https://eprints.whiterose.ac.uk/>

Annealing impact on mechanical performance and failure analysis assisted with acoustic inspection of carbon fiber reinforced poly-ether-ketone-ketone composites under flexural and compressive loads

Sinem Elmas^{1,2}  | Buse Atac^{1,2} | Cahit Orhun Senol^{1,2} | Serra Topal^{1,2} | Mehmet Yildiz^{1,2}  | Hatice S. Sas^{1,2,3} 

¹Faculty of Engineering and Natural Sciences, Sabanci University, Istanbul, Turkey

²Sabanci University Integrated Manufacturing Technologies Research and Application Center & Composite Technologies Center of Excellence, Pendik, Turkey

³School of Mechanical, Aerospace and Civil Engineering, The University of Sheffield, Sheffield, UK

Correspondence

Hatice S. Sas, Faculty of Engineering and Natural Sciences, Sabanci University, Orhanli-Tuzla, Istanbul 34956, Turkey.
Email: haticesas@sabanciuniv.edu

Funding information

Scientific and Technological Research Council of Turkey (TUBITAK), Grant/Award Numbers: 221M565, 218M709

Abstract

This study investigates the effect of the annealing treatment for carbon fiber reinforced Polyether-ketone-ketone (CF/PEKK) composite structures under flexural and compressive loadings through reference, pre-damaged, and annealed sample sets. Significant recovery of pre-existing damage is observed after the annealing process, following both flexural and compressive loading. Acoustic emission (AE) inspection is employed to monitor the failure behavior and assess the impact of pre-damage and annealing on CF/PEKK composite. Initially, AE inspection reveals that the reference CF/PEKK material exhibits a notable fiber-related failure with 85% of cumulative AE counts under flexural load, whereas matrix-related failures are more pronounced with 92% cumulative AE counts under compressive load. Pre-damages in the matrix alter the cumulative count percentages and initiation time that are related to matrix, interface, and fiber-related failures, under flexural and compressive loadings. After annealing, each cumulative AE count percentages are comparable to reference sample values, due to changes in microstructure and relieving of residual stresses. The annealing effect is further validated through dynamic scanning calorimetry (DSC) analysis results with increased glass transition temperature (T_g) and degree of crystallization (X_c). Overall, these findings indicate that annealing treatment effectively restores structural integrity and improves the mechanical performance of CF/PEKK composites.

Highlights

- Annealing aims for damage recovery in CF/PEKK under flexural and compressive loads.
- Significant damage recovery in CF/PEKK is seen after annealing.

This is an open access article under the terms of the [Creative Commons Attribution-NonCommercial-NoDerivs](https://creativecommons.org/licenses/by-nc-nd/4.0/) License, which permits use and distribution in any medium, provided the original work is properly cited, the use is non-commercial and no modifications or adaptations are made.

© 2024 The Author(s). *Polymer Composites* published by Wiley Periodicals LLC on behalf of Society of Plastics Engineers.

- Annealing raises T_g and crystallinity, and enhances CF/PEKK structural integrity.

KEYWORDS

acoustic emission inspection, annealing, mechanical characterization, thermoplastic composites

1 | INTRODUCTION

High-performance thermoplastic polymers are receiving increased attention in the aerospace industry for composite production. Thermoplastic composites (TPCs) provide several advantages over their thermoset counterparts, including compliance with aeronautical mechanical specifications, room-temperature storage, recyclability, and more efficient processing methods.^{1–3} PEKK is a semicrystalline polymer that belongs to the Poly Aryl Ether Ketone (PAEK) family, with a glass transition temperature (T_g) at 160°C, a moderate processing temperature (330–380°C), and high strength and stiffness.⁴ The combination of these characteristics makes PEKK highly suitable for manufacturing aerospace structures. The manufacturing of TPCs can be performed with autoclave consolidation, automated tape laying (ATL), automated fiber placement (AFP), compression molding, and vacuum-bag-only (VBO). Among these, the VBO process stands out as a fast and cost-effective manufacturing process compared to the traditional autoclave method. However, there are limited studies in the literature addressing the manufacturing challenges of VBO for TPCs, which face constraints due to limited vacuum pressure.⁵ Zhang et al.⁶ investigated void reduction during VBO processing for high-performance carbon fiber reinforced thermoplastic composites with varying thicknesses and presented the processing window for thick composites with low void content. In another study, Swamy et al.³ outlined the process design to promote air removal for CF/PEKK laminates by VBO consolidation.

Damage can occur both during the manufacturing of composite structures and throughout service life under various loading configurations. Manufacturing-related damages include porosity, voids, micro-cracks in the matrix, delamination, fiber waviness, interface debonding, surface gouges, drilling holes, and impact damage (e.g., dropped tools on the parts).⁷ Furthermore, composite structures are engineered to withstand a variety of loading types, with flexural and compression loads being notable examples. Each loading type induces specific failure modes, which are critical to the structural performance of aerospace structures, particularly during critical phases like takeoff, landing, turbulence, and maneuvers. Therefore, understanding the damage evolution in TPCs is a critical issue to ensure the safety and

reliability of service life, especially in cases where micro-cracks are introduced in the matrix, which can trigger catastrophic failure.⁸ In this regard, the AE method is a passive non-destructive evaluation (NDE) method generally employed to identify damage types and classify them, contributing to the understanding of damage formation and evolution in composite materials and structures under various loading conditions. This is achieved by recording temporary elastic waves caused by rapidly released energy due to the damage.⁹ Several studies have employed AE inspection to classify damage types in CF/PEKK composites under tensile loading. For example, Yildirim et al.¹⁰ characterized the damage evolution of CF/PEKK composites using AE and revealed that the tensile failure behavior transitions from matrix-dominant to fiber-dominant as the load increases. They further noted that the onset of fiber-dominated failure aligns with a gradual increase in the material stiffness under tensile loading, which was observed through clustering and analyzing AE hits and counts. Sukur et al.¹¹ highlighted accelerated aging on the damage mechanism of CF/PEKK composites under tensile load and they demonstrated that the clusters of matrix cracking and interface failures increased after 30 days of hot-wet aging. They associated this rise with inhibiting the motion of polymer segments. However, a comprehensive examination of the damage evolution on the CF/PEKK composite under different load configurations, specifically for flexural and compressive loads, has yet to be conducted using acoustic emission inspection.

Repair methods are crucial for restoring damage and preserving the overall structural integrity of composite materials. When compared to replacing damaged parts entirely, employing repair techniques proves to be a more cost-effective solution. TPCs possess the unique capability to remelt and reform within a short timeframe, making them responsive to repair through the application of heat. Crucial techniques in the repair process of TPCs include welding methods, that entail applying heat to the damaged area, partially melting the matrix in the interface region, and fusing the damaged region.⁷ However, welding methods are generally suited for the localized repair of damaged areas in composite structures and may not effectively address widespread damages that occur within the structure.¹² To address the healing of more extensive

damage types like matrix cracking and delamination, annealing emerges as a significant thermal treatment process. Annealing is conducted above the glass transition temperature (T_g) and below the melting temperature (T_m) of the semicrystalline thermoplastic matrix, and it facilitates the reduction of residual effects from manufacturing and operational activities by increasing crystallinity, hence enhancements in structural performances of the material.¹³ For instance, Regis et al.¹⁴ demonstrated an increase in the crystallinity degree of carbon fiber reinforced poly-ether-ether-ketone (CF/PEEK) from 32.3% to 33.7% through annealing at 200°C. Their flexural tests revealed a significant correlation between mechanical properties and the rise in crystallinity, with the maximum flexural load showing improvement post-annealing. Similarly, Yu et al.¹⁵ applied annealing heat treatment at 150°C, slightly above the T_g , for 60 min to 3D-printed CF/PEEK laminates. This resulted in an increase in crystallinity from 11.3% to 13.8% and subsequently enhanced interlaminar shear strength values, reflecting a 16% recovery. Thus, the annealing process facilitated increased mobility of PEEK molecular chain segments, leading to enhanced interlayer bonding strength. Moreover, a gradual increase in mechanical properties was observed with increasing annealing temperatures, up to T_m . While many previous studies have primarily treated annealing as a post-manufacturing process, it holds significant potential as an effective repair method for addressing widespread matrix damage that occurs during the manufacturing or operation of large-scale thermoplastic composite structures. Conejo et al.¹⁶ demonstrated that applying thermal treatment by hot-press to CF/PAEK composites after impact, restored compression strength. Samples impacted with 5 J returned to their original strength, while those impacted with 10 and 30 J showed partial recovery. Despite its potential, the literature lacks sufficient exploration of the impact of annealing treatment on damage healing in thermoplastic composites, including mechanical characterization and failure mechanisms.

This study aims to investigate the effect of annealing on pre-existing damages in TPCs and to gain insight into their mechanical and fracture behavior, leveraging AE inspection of CF/PEKK composites manufactured through the VBO process. To the best of the authors' knowledge, a comprehensive investigation has not been previously undertaken in the literature. To achieve this goal, pre-damages are induced into composite samples by applying pre-determined loads identified through acoustic emission inspection. Subsequently, the pre-damaged samples undergo annealing. Void content and DSC analyses are conducted to assess the microstructural and thermal quality of the VBO-manufactured thermoplastic composite,

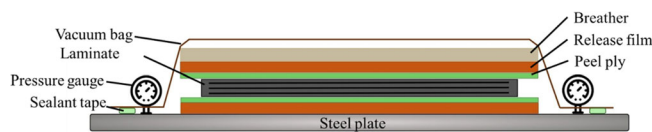


FIGURE 1 Schematic illustration of vacuum-bag-only (VBO) process.

respectively. Three-point bending and compression tests are performed to analyze the impact of pre-damage and annealing treatment on the mechanical performance of the CF/PEKK samples. An in-situ damage monitoring method, AE inspection, is employed during mechanical tests to comprehensively understand the damage mechanism of the reference, pre-damaged, and annealed CF/PEKK composite samples.

2 | EXPERIMENTAL PROCEDURE

2.1 | Materials

Toray Cetex[®]TC1320 carbon fiber reinforced poly-ether-ketone-ketone (CF/PEKK) unidirectional tape, sourced from Toray Advanced Composites, USA, is used for composite laminate manufacturing. The tape boasts a nominal thickness of 0.15 mm and a width of 305 mm. It features a resin content of 34% by weight, a fiber areal weight (FAW) of 145 g/m², a prepreg areal weight (PAW) of 221 g/m², and requires a processing temperature of 370°C.¹⁷

2.2 | Manufacturing of composite laminate

In this study, firstly the CF/PEKK tapes are cut in the dimensions of 110 × 310 × 3.2 ± 0.2 mm³ using a digital cutting machine (ZÜND G3-L3200). CF/PEKK laminates are fabricated by the VBO process, as illustrated in Figure 1. The layup configuration of laminates follows a quasi-isotropic and symmetric pattern with a stacking sequence of [0/45/90/(-45)₂/90/45/(0)₂/45/90/-45]_s. Before the layup process, a release agent (Loctite Frekote 700-NC) is sprayed onto the steel plate and allowed to set for 30 min. Subsequently, a polyimide perforated release film, UPILEX[®] 25S is placed on the top and bottom of the composite laminate to facilitate easy release. Following these preparatory stages, the lamination of composite tapes is laid up in quasi-isotropic configurations as mentioned above. Woven glass fabric Bleeder Lease[®] E-peel ply is positioned at the bottom and top of the composite laminate. Additionally, the Airweave[®] UHT800 nonwoven ultra-high temperature fiber-glass breather is introduced on top of the perforated release

film to aid in air evacuation and sustain vacuum levels. Finally, the laminate is covered with Thermalimide E polyimide film and securely sealed using A-800 3G sealant tape, making it ready for place into the oven as described by Swamy et al.³

Before being placed into the oven (Sistem Teknik—CCO-800-1461-1804) the vacuum of the layup is set at 1 atmosphere (atm) and maintained for 24 h debulking. Subsequently, the prepared vacuum bag layup is placed in the oven after keeping the preform under vacuum for 24 h and exposed to a heating cycle, with the vacuum pump set at 1 atm to maintain constant pressure during the process. The oven temperature gradually increased to 250°C at a heating rate of 4°C/min. Subsequently, a further increment to 378°C is applied at a rate of 3°C/min.¹⁸ The laminates are kept at this elevated temperature for a dwell period of 90 min.³ Then, the temperature is lowered to room temperature at a constant cooling rate of 3°C/min.

2.3 | Material and thermal characterization

The density of the CF/PEKK composite sample is determined by ASTM D792/Method A, based on the water buoyancy (SHIMADZU-AUX220), following Archimedes' principle. To analyze the void content and fiber volume fraction of the CF/PEKK samples, ASTM D3171/Method B is employed, involving two samples sized at 25 × 25 mm², subjected to matrix digestion with acid treatment in the three-neck glass flask. The void content is calculated using the relations provided in Equation (1)¹⁹;

$$V_v = 100 - (V_f + V_m) \text{ with}$$

$$V_f = \frac{M_f}{M_i} \times \frac{\rho_i}{\rho_f} \times 100 \text{ and}$$

$$V_m = \frac{M_i - M_f}{M_i} \times \frac{\rho_i}{\rho_m} \times 100$$
(1)

where V_f , V_m , and V_v are the volumetric percentages (%) of the fibers, matrix, and voids in the composite accordingly. M_f , and M_i are the mass (g) of the sample after digestion, and the mass of the sample before digestion. ρ_f , ρ_m , and ρ_i are the densities (g/cm³) of the fibers, matrix, and the sample, respectively.

Optical microscopy images are captured using Nikon—LV100ND metal microscopy to analyze the void content and their distribution in the composite laminates. Samples are molded in epoxy (BUEHLER-VariDur200) and prepared for cross-sectional analysis, with surface polishing performed to improve image clarity. Furthermore, after conducting mechanical tests, the optical

microscope is utilized to examine the fracture surface of the composite samples.

DSC measurements are performed by using the Mettler Toledo DSC⁺ analysis instrument in order to determine the degree of crystallization and thermal behavior of the CF/PEKK composites. All DSC experiments are carried out under an inert nitrogen (N₂) atmosphere with a flow rate of 50 mL/min, within a temperature range of 25–400°C with a heating/cooling rate of 10°C/min. The X_c is calculated based on the melting enthalpy of the composite and melting enthalpy corresponding to PEKK material with 100% crystallinity (130 J/g), with the following equation²⁰;

$$X_c = \frac{\Delta H_m}{\Delta H_m^0 \times W_m} \times 100$$
(2)

where ΔH_m is the melting enthalpy obtained from DSC measurement, ΔH_m^0 is the melting enthalpy of PEKK resin with 100% crystallinity, and W_m is the matrix weight fraction in the composite sample.

2.4 | Mechanical characterization and damage analysis

To evaluate the mechanical properties of CF/PEKK laminates, three-point bending, and compression tests are performed following ASTM D790 and ASTM D6641 standards, respectively. The Instron 5982 Universal Testing Machine, equipped with a static load cell of ±100 kN (as shown in Figure 2A,B), is employed for testing. Samples, measuring 12.7 mm in width, 61.5 mm in height, and with a thickness of 3.2 ± 0.2 mm for bending samples, and 140 mm × 13 mm × 3.2 ± 0.2 mm³ for compression samples. The cross-head speed is set to 1.3 mm/min during the tests. The combined loading compression (CLC) method²¹ applies both end- and shear loading to the sample which ensures reliable results by preventing the crushing of sample ends, thus eliminating the need for repetitive testing.

In this study, the three-point bending and compression tests are complemented by AE inspection to provide detailed damage detection. Additionally, AE analysis is used to determine the optimal pre-load levels to generate pre-damage under flexural and compression loadings. AE serves as a non-destructive testing method, involving the detection and analysis of transient stress waves or acoustic signals generated within a material during deformation or damage.⁹ Throughout the mechanical characterization experiments, AE data are continuously captured using a system equipped with two wideband piezoelectric sensors (PICO-200–750 kHz, Mistras) and AEwin PCI2

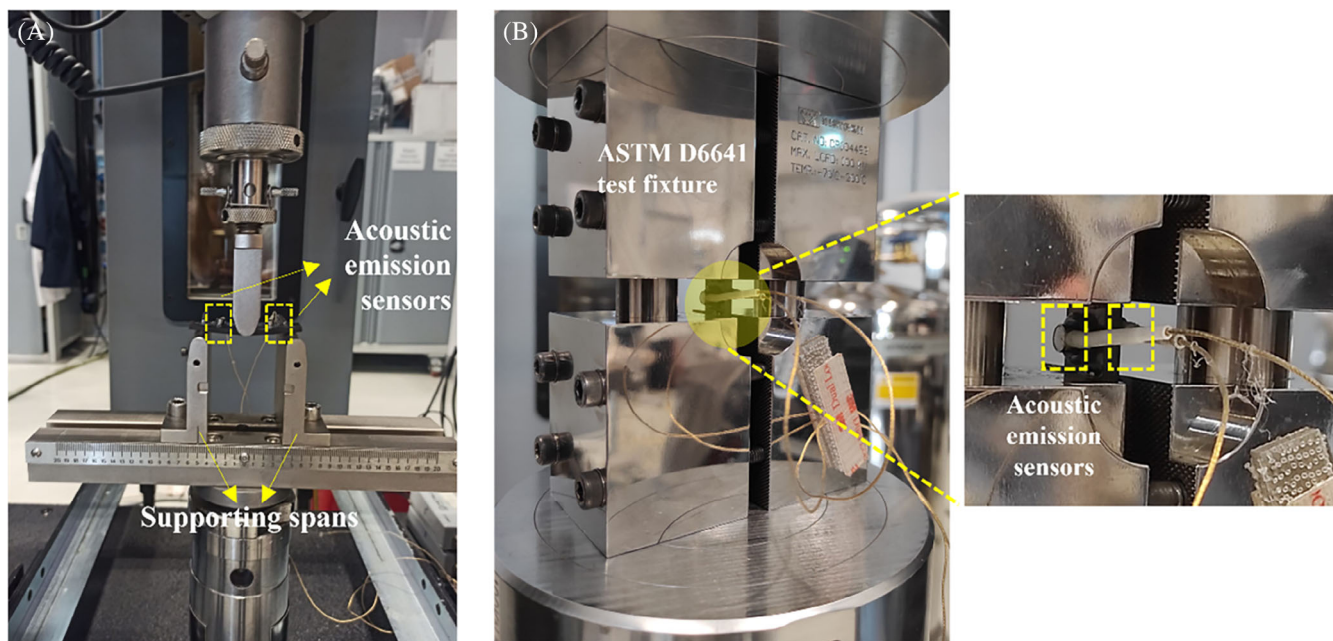


FIGURE 2 The mechanical test setups for (A) three-point bending and (B) compression tests with corresponding acoustic emission sensor placements.

software. These sensors are mounted on the composite laminates during tests at an equal distance from the supporting spans as shown in Figure 2A,B for three-point bending and compression tests, respectively. The Physical Acoustics 0/2/4 voltage preamplifier is employed to output a signal with an enhancement (gain) of 20 dB in a single mode. The data acquisition parameters are set to a threshold value of 40 dB, a peak definition time (PDT) of 50 μ s, and a hit definition time (HDT) of 150 μ s. The hit lockout time (HLT) parameters are adjusted at 200 and 300 μ s for flexural and compression tests, respectively, in order to collect data efficiently.^{10,11} The Bessel band-pass filter, operating within the frequency range of 20 to 800 kHz, is employed for noise mitigation in the acquired signals. Examination of the temporal distribution of acoustic emission signals reveals a scarcity of AE activity during the initial phase of linear deformation. However, during the intermediate and concluding stages of linear deformation, the occurrence and amplitude of AE signals manifest a notable and progressive augmentation over time. The post-processing of acoustic emission signals involves the utilization of Noesis 7 software to extract waveforms. Subsequently, the clustering of acoustic events is executed through a MATLAB script. The determination of the optimal number of clusters corresponding to distinct damage types is conducted by employing the Calinski-Harabasz criterion,²² considering both the amplitude and peak frequency of the collected acoustic data. The k-means clustering algorithm is applied to categorize the acoustic events,

wherein each data point is assigned to the cluster with the nearest mean.²³

2.5 | Annealing treatment

Annealing is a heat treatment process commonly used for improving the mechanical properties and stability of material.²⁴ Annealing can be carried out by increasing the temperature of the composites above the glass transition temperature (T_g) and below the melting temperature (T_m) of the matrix. The annealing temperature, time, and cooling are important to increase the mobility of polymer chains and recrystallization.^{25,26} During the heating and dwell time, the molecular chain relaxation occurs and enables the realignment of the chains.²⁷ During the cooling, polymer chains lose mobility, they rearrange into ordered crystalline structures through nucleation and growth processes which leads to an improvement in the degree of crystallinity.^{26,28} Additionally, increased molecular mobility promotes stronger interfacial bonding and reduces the presence of voids or weak points between the fiber and matrix. Also, relaxation of residual stresses occurs during annealing treatment, and internal stresses, accumulated during manufacturing and previous loadings, are relieved.²⁵ By increasing crystallinity and reducing residual stresses, annealing not only improves the bulk mechanical properties but also strengthens the fiber-matrix interface. These changes, enhancement of the crystallinity level of the

thermoplastic matrix, induce a decrease in residual effects within the material, directly contribute to the mechanical properties. Increased crystallinity enhances strength, while stress relaxation contributes to the composite's ability to recover from pre-existing damage. The bonding between fibers and the matrix in the composites is fundamental to efficient load transfer. A strong interfacial bond ensures that the stress applied to the composite is effectively distributed between the fiber and matrix, minimizing the risk of matrix cracking, fiber pull-out, or delamination under mechanical loads.²⁹ Therefore, the thermoplastic composite samples are exposed to an annealing process within an oven to mitigate pre-damages that are induced in the sample and recover any adverse mechanical effects that may be present. In this study, the pre-damaged samples are annealed in an oven (Pol-Eko-Aparatura—SLW 115 IG SMART) for one hour dwell time at 180°C. The maximum temperature is selected at 20°C higher than the glass transition temperature of PEKK resin¹⁵ and the heating and cooling rates are set at 8°C/min. Afterward, DSC and mechanical analyses are repeated at the same conditions for the annealed samples.

3 | RESULTS AND DISCUSSION

3.1 | Void content analysis

The void content of the CF/PEKK composite laminate is determined based on the densities of composite laminate, matrix, and fiber. The densities of UD carbon fiber and PEKK matrix are 1.79 and 1.30 g/cm³, respectively. The density of the composite laminate is calculated as 1.57 g/cm³ using ASTM D792/Method A. The weight

percentages of fiber (W_f) and matrix (W_m) are measured at $65.65 \pm 0.11\%$ and $34.35 \pm 0.11\%$, respectively, according to ASTM D3171/Method B standard. Subsequently, void content is calculated as $0.61 \pm 0.18\%$ using Equation (1).

3.2 | Thermal characteristics of the CF/PEKK composite and the effect of the annealing treatment

In this study, the impact of annealing on the thermal properties of CF/PEKK composites is assessed, focusing on parameters such as the T_g , crystallization temperature (T_c), melting temperature (T_m), and X_c . The DSC traces of reference and annealed CF/PEKK samples are presented in Figure 3 and the findings of the DSC analyses are tabulated in Table 1. In Figure 3A, T_g from the heating curves of reference and annealed samples are determined as 155.59 and 160.93°C, respectively. This result can be associated with the annealing of the composite above the T_g inducing partial melting and recrystallization. Thereby, the chain mobility of the amorphous region is restricted by the crystalline region, and thus, an increase in the T_g value is observed due to the more arranged crystalline region.³⁰ The cooling curves given in Figure 3B present the crystallization temperature of both samples. The heating and cooling graphs in Figure 3 show similar behavior in T_m , and T_c for reference and annealed samples. Moreover, the annealed sample demonstrates an X_c of 21.61%, indicating a rise compared to the reference sample, which possesses a degree of crystallinity of 19.70%, calculated using Equation (2). The increase in the X_c is also supported by x-ray diffraction (XRD) analysis results with an increase in intensity after

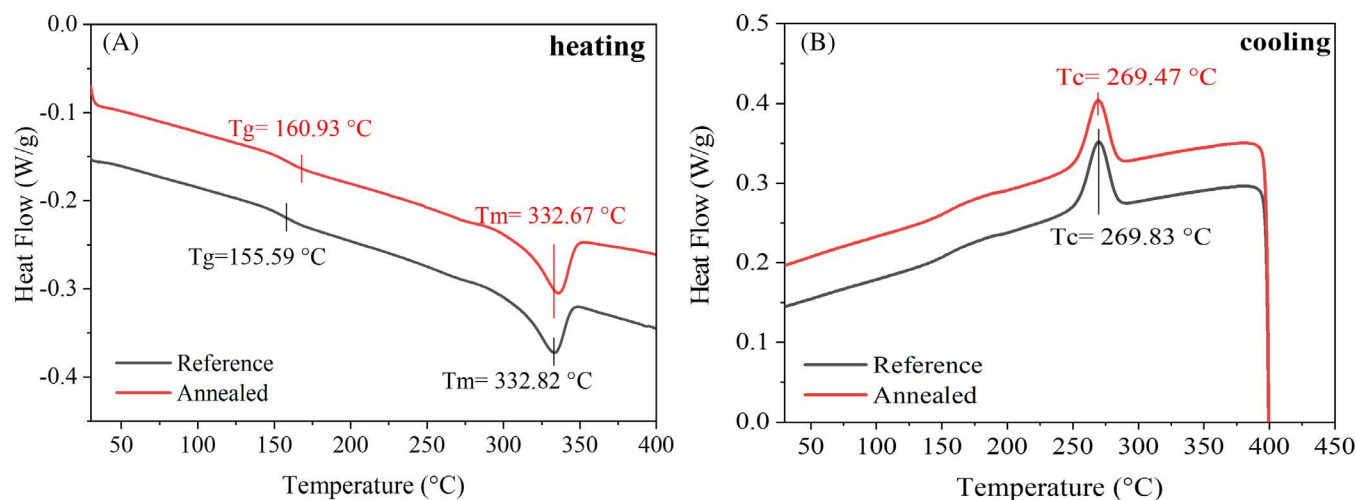


FIGURE 3 DSC curves of CF/PEKK and annealed CF/PEKK composites for (A) the heating, and (B) the cooling.

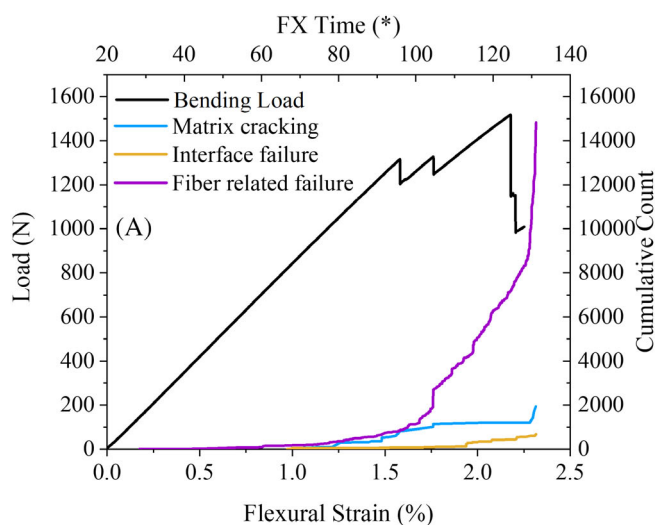
annealing³¹ as given in Figure S1. The increase in X_c can be explained by the influence of the migration of chain segments and reordered again during heating higher than the T_g value of matrix material with annealing.^{30,32} Meanwhile, the low increase in crystallinity value can be attributed to annealing temperature since it influences the crystallization process in thermoplastics.^{24,25}

3.3 | Optimum pre-loads for pre-damage generation under flexural and compression loadings

First, a set of three-point bending and compression tests are performed with AE inspection assistance to determine the optimal pre-load levels to generate pre-damage in the form of micro-cracks, primarily through matrix crack dominant failure types. Figure 4 represents the force and strain curves for the three-point bending (Figure 4A) and compression (Figure 4B) tests assisted with AE inspection. In the context of both tests, the optimal number of clusters is identified as three addressing matrix, interface, and fiber-related failures. Leveraging this predetermined cluster count, the k-means clustering algorithm is applied to categorize the acoustic events,

TABLE 1 DSC analyses results of reference and annealed CF/PEKK samples.

	T_g (°C)	T_c (°C)	T_m (°C)	ΔH_m (J/g)	X_c (%)
Reference	155.59	269.83	332.82	8.80	19.70
Annealed	160.93	269.47	332.67	9.65	21.61



wherein each data point is assigned to the cluster with the nearest mean.²³ For the three-point bending test (Figure 4A), the cumulative counts of AE data show that failure starts higher than 1.25% strain level, and, a sudden increase in all failure types is observed after a strain level of 2%. Thus, the amount of pre-load for the pre-damage generation into three-point bending samples is selected as 1200 N which corresponds to a strain within the range of 1.25% and 2%. For the compression test (Figure 4B) the matrix crack dominated failure initiation starts at a strain level of 0.25%, while the interface and fiber-related failures are observed beyond the 1% strain level. Thereby, the pre-load for the compression test to introduce a pre-damage is assigned as 19,000 N into the compression test samples. Consequently, mechanical tests are conducted on three samples: reference, pre-damaged (representing the application of pre-loads as provided in Section 2.4), and annealed (representing the annealed pre-damaged samples following the procedure given in Section 2.5).

3.4 | Three point bending test results

The flexural performance of reference, pre-damaged, and annealed samples is assessed using the ASTM D790 standard, supplemented by AE inspection (Figure 5). In the analysis of flexural test outcomes, a consistent fracture behavior characterized by a decline followed by an increase in stress is observed across all samples (Figure 5A). This behavior is attributed to the quasi-isotropic layup sequence of the laminates, which influences the mechanical response during bending.³³ Specifically, the observed stress pattern is primarily attributed to delamination failure occurring between

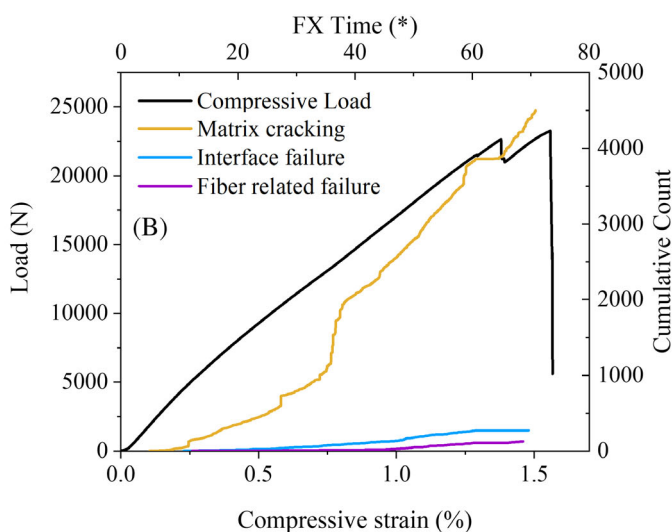


FIGURE 4 AE results with load-strain curves for (A) three point bending, (B) compression tests.

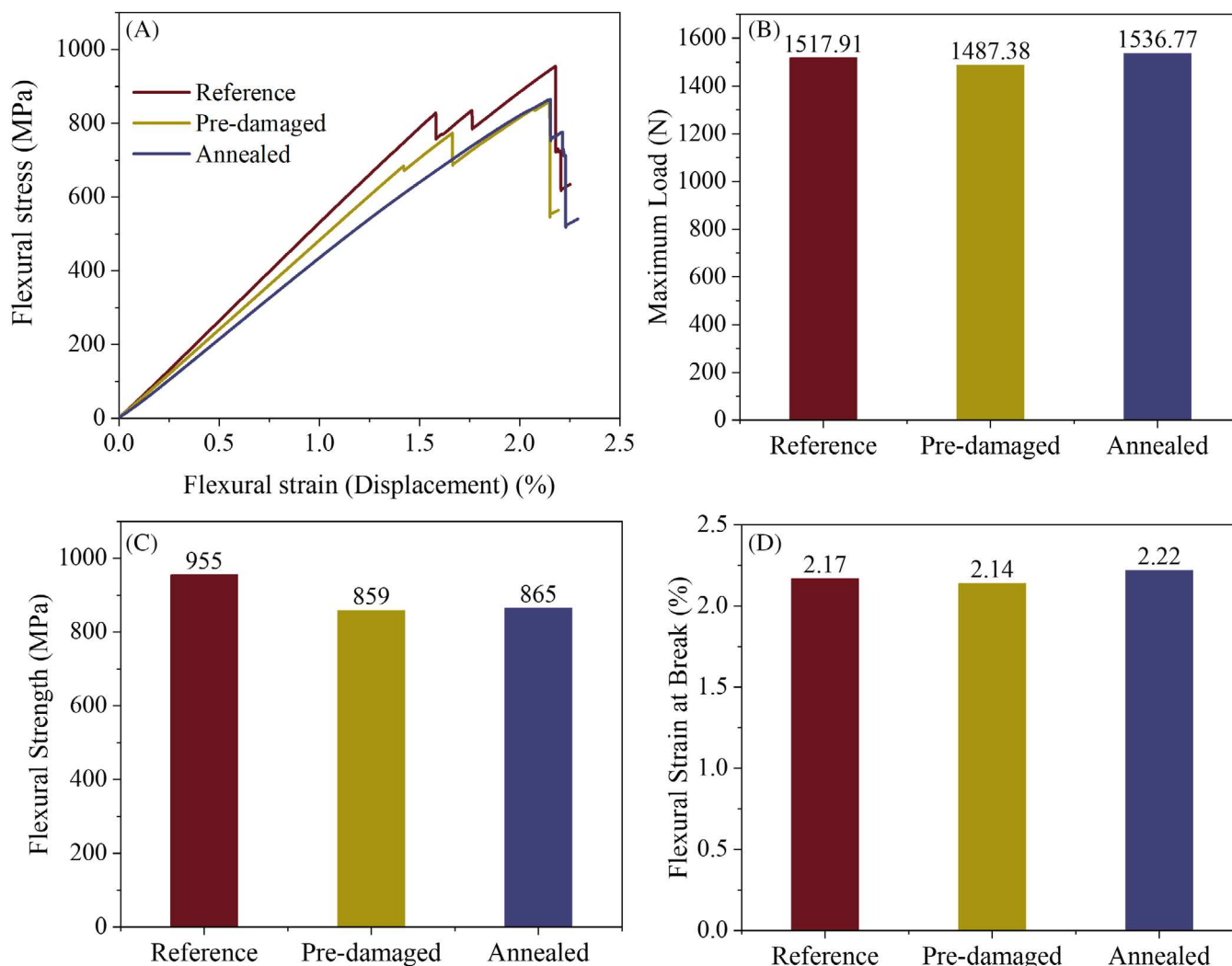


FIGURE 5 Three-point bending test results for CF/PEKK samples with reference, pre-damaged, and annealed configurations with (A) representative flexural stress–strain curves and (B–D) bar charts for maximum load, flexural strength, and flexural strain at break, respectively.

layers with different fiber orientations within the composite laminates.³⁴ The presence of delamination, a critical failure mode in laminated composites, underscores the importance of understanding and mitigating interlaminar defects to enhance structural integrity and mechanical performance. As the applied load increases during the experiment, the samples initially fracture upon reaching a critical load, after which the stress value decreases. Subsequent loading shows a slight decline in stress, followed by a subsequent increase, eventually reaching another critical load point. At this point, the stress value rises again, leading to the fracture of the sample that has reached its maximum load. This behavior highlights the complex response of the material to increasing loads, characterized by multiple stages of stress fluctuation and ultimate failure under progressively higher loads which are reported in the quasi-isotropic [45/0/−45/90]_{2s} laminate of carbon fiber/polyamide 6 by Uematsu et al.³⁵ The three

point bending test results are also compared for the maximum load (Figure 5B), flexural strength (Figure 5C), and flexural strain at break (Figure 5D). The reference composite exhibits a load capacity of 1517.91 N, with pre-damage induction the maximum load capacity decreases to 1487.38 N as seen in Figure 5B. However, annealed composite samples exhibit the maximum load capacity, reaching 1537.77 N. This enhancement is attributed to the relief of residual stresses, resulting in improved bonding between the matrix and reinforcing components, consequently enhancing the load-bearing capability.³⁶ The reference sample exhibits the highest flexural strength with a strength value of 955 MPa (Figure 5C). The flexural strength of pre-damaged sample decreases by 10% compared to the reference sample. It is likely that the applied pre-load forms micro-cracks in the PEKK matrix. These micro-cracks induce high local

stresses in the composite, leading to a decrease in the flexural strength of the material.³⁷ The annealed sample shows improvement in strength compared to the pre-damaged samples but does not fully recover the original properties of the reference composite. Despite the potential of annealing to promote healing, larger or more complex damages may not be fully recovered, and some residual damages may persist, limiting the material's ability to return to its original strength. Nevertheless, a notable shift is observed in the higher strain value of the annealed sample with the sample failing around the 2.22% strain level as seen in Figure 5D, indicative of a more ductile behavior. Moreover, a smoother stress-strain curve is observed in the annealed sample (Figure 5A) which is attributed to the reduction in the intensity of micro-cracks through the annealing treatment.

TPCs are complex materials with a combination of fibers and matrix. Achieving a restoration of the original properties involves intricate interactions between these components, and any deviation from the original configuration may affect the final mechanical performance. In order to better understand the effect of damages in the composite and annealing treatment, all experiments are characterized by the AE inspection method. The AE results of three point bending samples that represent each frequency range corresponding to the damage types are given in Figure 6 for reference, pre-damaged, and annealed CF/PEKK composites, respectively. Using the k-means clustering algorithm, the optimal number of clusters is identified as three for all samples. The lowest frequency range of peak frequency is due to damage initiation or its propagation in the resin matrix, in all the recorded AE data,¹¹ so the first cluster in the 0–230 kHz frequency range is attributed to cracking in the resin matrix.³⁸ The remaining two frequency ranges are consequently related to other damage types. The intermittent frequency range (420–480 kHz) is associated with the fiber/matrix interface failure, as defined previously in the literature.^{39,40} The third cluster in the frequency range (480–600 kHz) corresponds to the fiber-related failure for all samples under flexural load⁴¹ for all of the CF/PEKK three-point bending samples (Figure 6).

The AE analysis results are given as cumulative acoustic counts and stress-strain graphs for reference, pre-damaged, and annealed samples in Figure 7. The cumulative acoustic counts show that the flexural failure mechanism of all samples exhibited a dominant fiber-related failure mode. This suggests that the flexural performance of the composite is largely influenced by the quality of the fiber. For the reference sample, as the applied load increased during the experiment, the initial fracture in the sample takes place upon reaching a

critical load and then the stress value decreases at a strain value of 1.58%. This drop is attributed to matrix cracking, which predominately occurs up to this strain level, stabilizing, and remaining almost constant afterward, as depicted in Figure 7A. Further loading reveals a slight decline in stress, followed by an increase, eventually arriving at another critical load point at a strain level of 1.76%. At this time, a steeper rise in the fiber-related cumulative counts is observed. This increase corresponds to a rise in the flexural stress-strain curve. Subsequently, the stress value increases again, leading to the fracture of the sample at its maximum load. At this stage, failures related to fibers and interfaces are dramatically increased. Additionally, the sudden increase in interface failure indicates some level of debonding or separation between the carbon fibers and the PEKK, leading to sample failure. This finding is also observed from the optical microscopy images of fracture surfaces. The delamination failure occurred between the outer 0° and ±45° layers due to the interlaminar shear stress in the form of debonding and fiber breakage that arises between these layers under bending load (Figure 8A).²³

In the pre-damaged sample, there is a significant change in the percentage of the cumulative acoustic counts. While fiber-related failure remains the dominant failure type, the cumulative counts of the matrix cracking and interface failure are increased to 29.3% and 8.3%, from 11% and 4%, respectively compared to the reference sample. These significant increases indicate that the applied pre-load creates micro-cracks in the matrix. These micro-cracks lead to the formation and propagation of macro-cracks under flexural load and significantly affect the damage mechanism. The plastic deformation starts at a low strain value of 1.42%. This is shown as a significant rise in matrix cracking in the acoustic emission results as given in Figure 7B. Additionally, another drop in strength drop is observed at lower strain values at 1.65% and the sample failed at a strain value of 2.14%. The second stress drop is caused by the starting of interface failure and a slight increase in fiber-related failure. Similar to the reference sample fiber-related and interface failures are dominant and the matrix cracking is almost constant until the failure with higher cumulative counts of interface failure compared to the reference sample. As shown in Figure 7B, the cumulative acoustic counts of matrix cracking started at the onset of the loading which indicates the pre-damages made prominent matrix cracking at the early stages of the test. Transverse matrix cracks are formed by merging micro-ones as shown in the optical microscopy images in Figure 8B. McElroy et al.⁴² have mentioned a similar behavior of crack formation between different layers after being subjected to a biaxial-bending of the carbon fiber reinforced epoxy laminates. These transverse matrix cracks are the reason for the decrease of the load-

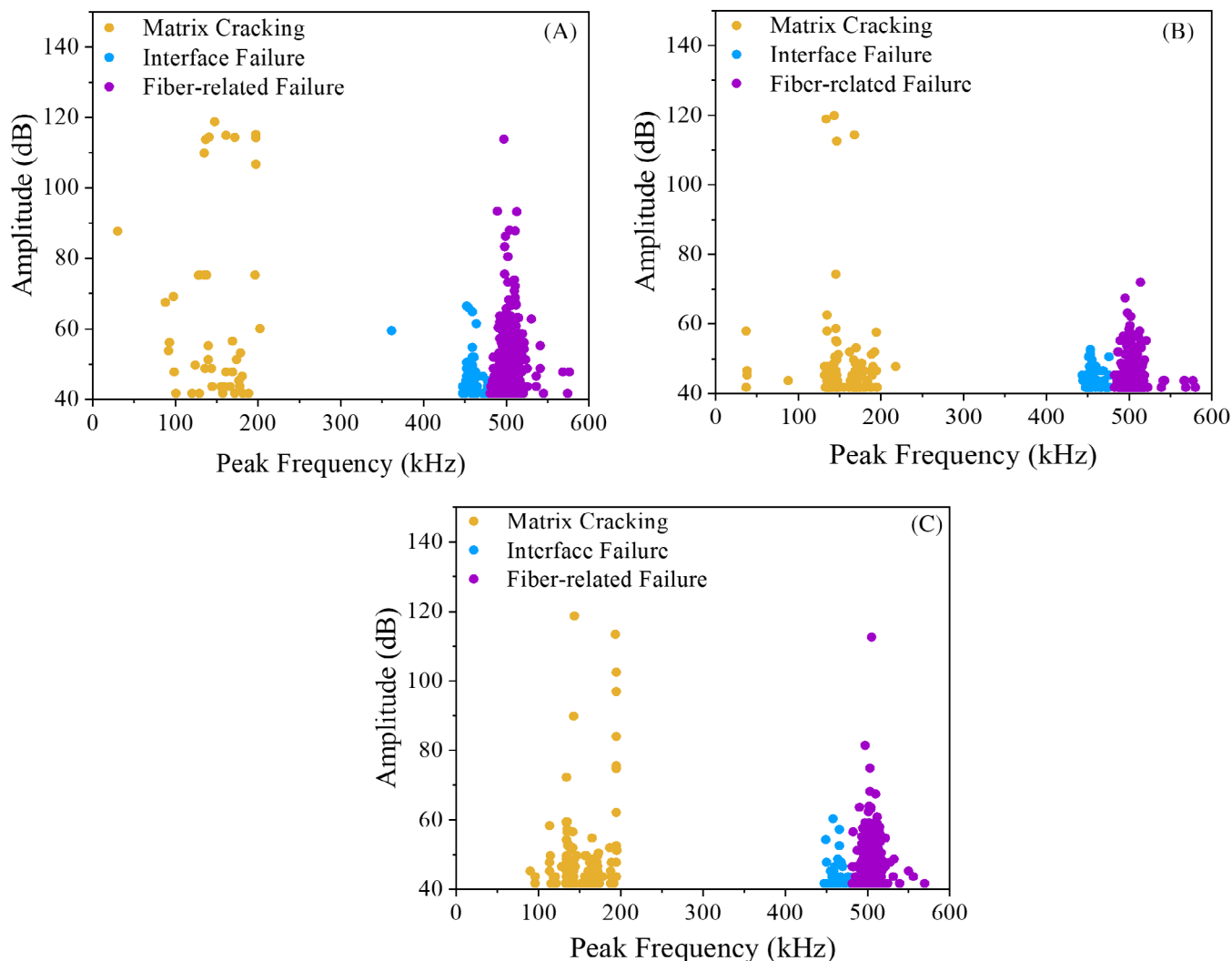


FIGURE 6 Clustered AE results of three point bending tests for each damage type with peak amplitude and peak frequency graphs for (A) reference, (B) pre-damaged, and (C) annealed CF/PEKK composite samples.

carrying capacity in the through-thickness direction and flexural strength.

Lastly, in the annealed sample the cumulative counts of matrix cracking and interface failure are decreased to 28% and 3%, respectively, which demonstrates the improvement in the bonding between carbon fiber and matrix with the aid of to annealing process. The starting point of the cumulative count curves of matrix cracking and interface failure is delayed compared to the pre-damaged sample. This indicates the healing of the matrix as a consequence of heat treatment. However, fiber-related failure started earlier and the cumulative count percentages increase to 69% from 62.4% compared to the pre-damaged sample. Similar to the reference sample, the first acoustic signals belong to fiber-related failure. It can be stated that the strength drop is postponed by the annealing effect and results in a smoother shift in the fracture behavior compared with the pre-damaged sample. As seen in

Figure 7C, there is no sudden increase in matrix cracking and fiber-related failure likely reference and pre-damaged sample. Nevertheless, the cumulative counts for interface failure start near the failure point and rise abruptly. Therefore, a shift is observed in the higher strain values of each stage compared to reference and pre-damaged samples and the sample failed around 2.22% strain level which indicates a more ductile behavior. The smoother stress–strain curve can be associated with eliminating the pre-damages during annealing treatment. The reduced intensity of the transverse cracks is highlighted with marks on the microscopy images of the annealed sample in Figure 8C. This indicates that the effect of the micro-cracks in the matrix is largely mitigated as a result of annealing treatment. As a consequence, after the annealing treatment, an improvement in flexural strength is observed compared to the pre-damaged sample, and most importantly the damage mechanism recovered similarly to reference samples.

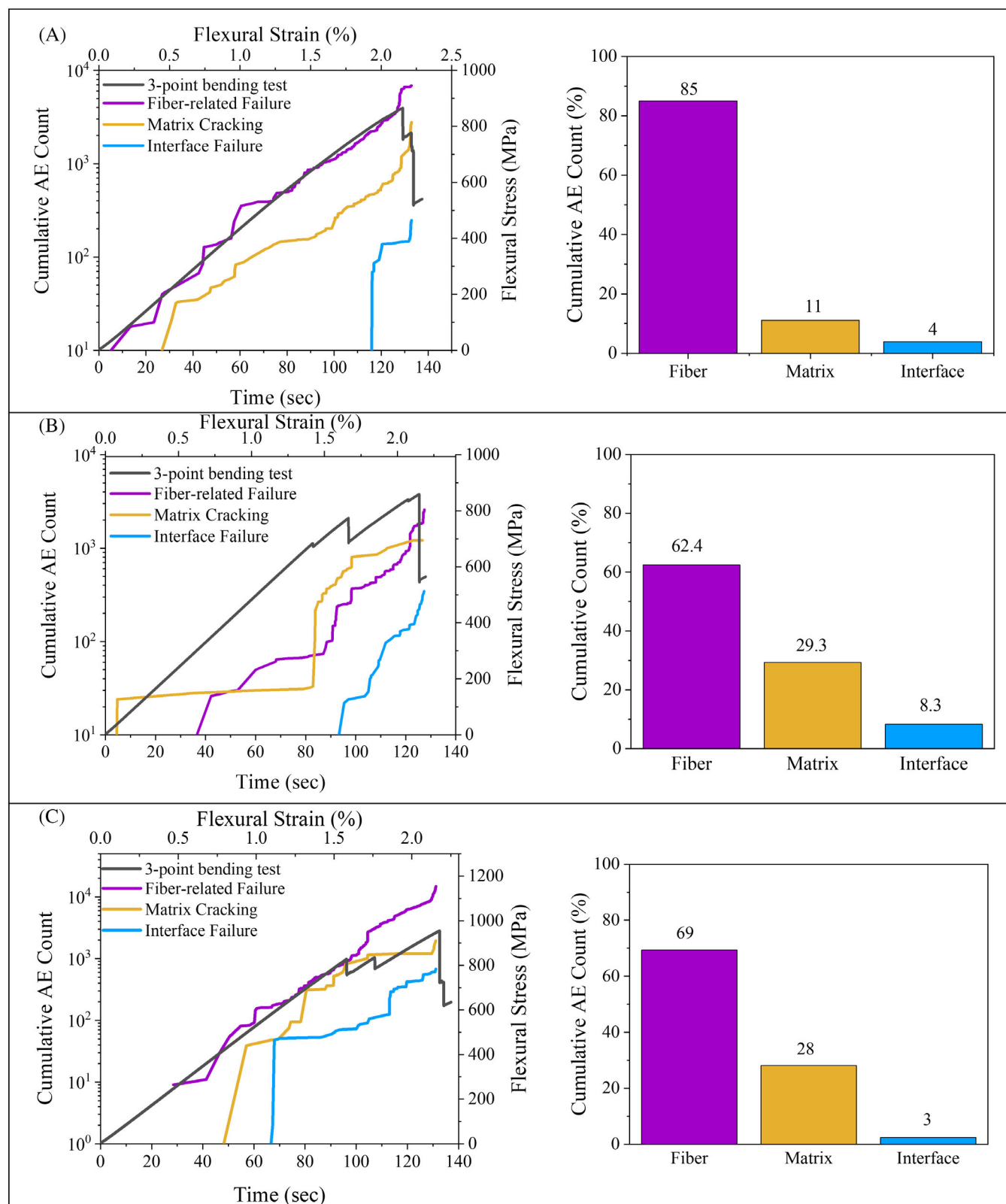


FIGURE 7 Cumulative AE count curves with three-point bending stress–strain curve alongside percentage failure type distributions (fiber-related, matrix cracking, interface failure) for (A) reference, (B) pre-damaged, (C) annealed CF/PEKK composite samples (The AE counts correlate failure mechanisms with stress–strain behavior under bending, showing the percentage distribution of each failure type at maximum strain)

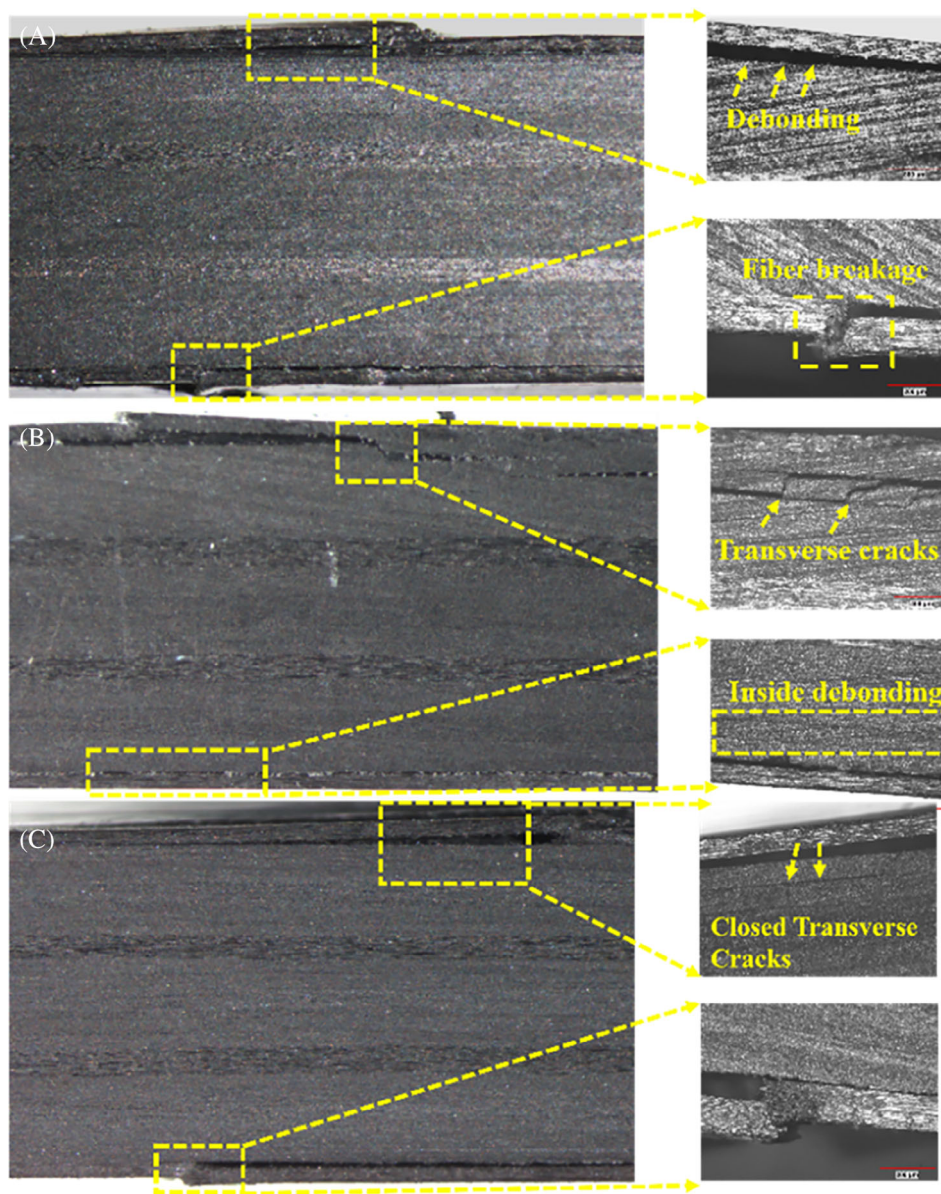


FIGURE 8 Optical microscope images after three-point bending test of (A) reference, (B) pre-damaged, (C) annealed CF/PEKK composite samples.

3.5 | Compressive test results

The compressive stress–strain curves, and bar charts for maximum load, compressive strength, and strain values of reference, pre-damaged, and annealed CF/PEKK samples are given in Figure 9. Two distinct stages are observed in the stress–strain curve of the reference sample (Figure 9A). The initial decrease in stress can be attributed to the failure of the outer fibers. However, stress recovery occurs following the onset of the first delamination attributed to symmetrical layers in the composite laminate.⁴³ The sample lost its structural integrity due to delamination of the inner layers, leading to ultimate failure. In contrast, the single-stage failure in the stress–strain curve of the pre-damaged sample can be attributed to brittle fracture. The annealing process

enhanced the compression stiffness of the CF/PEKK sample by eliminating pre-damages. Additionally, the elastic region extends to higher strain values are compared to the reference and pre-damaged samples, primarily due to the reduction of residual stresses in the matrix achieved through annealing.⁴⁴ Some fluctuations are observed in the stress–strain curve of the annealed sample at a strain value of 1.40%, potentially due to incomplete recovery of pre-damage compared to the reference sample. The reference samples present the maximum load capacity under compressive loading with a value of 23266.71 MPa. As expected, the load capacity decreased to 21194.08 MPa in the pre-damaged sample and increased after annealing treatment (Figure 9B). Consequently, the compressive strength of the CF/PEKK sample decreased by 7.66% as the pre-damage induced and, followed by an enhancement

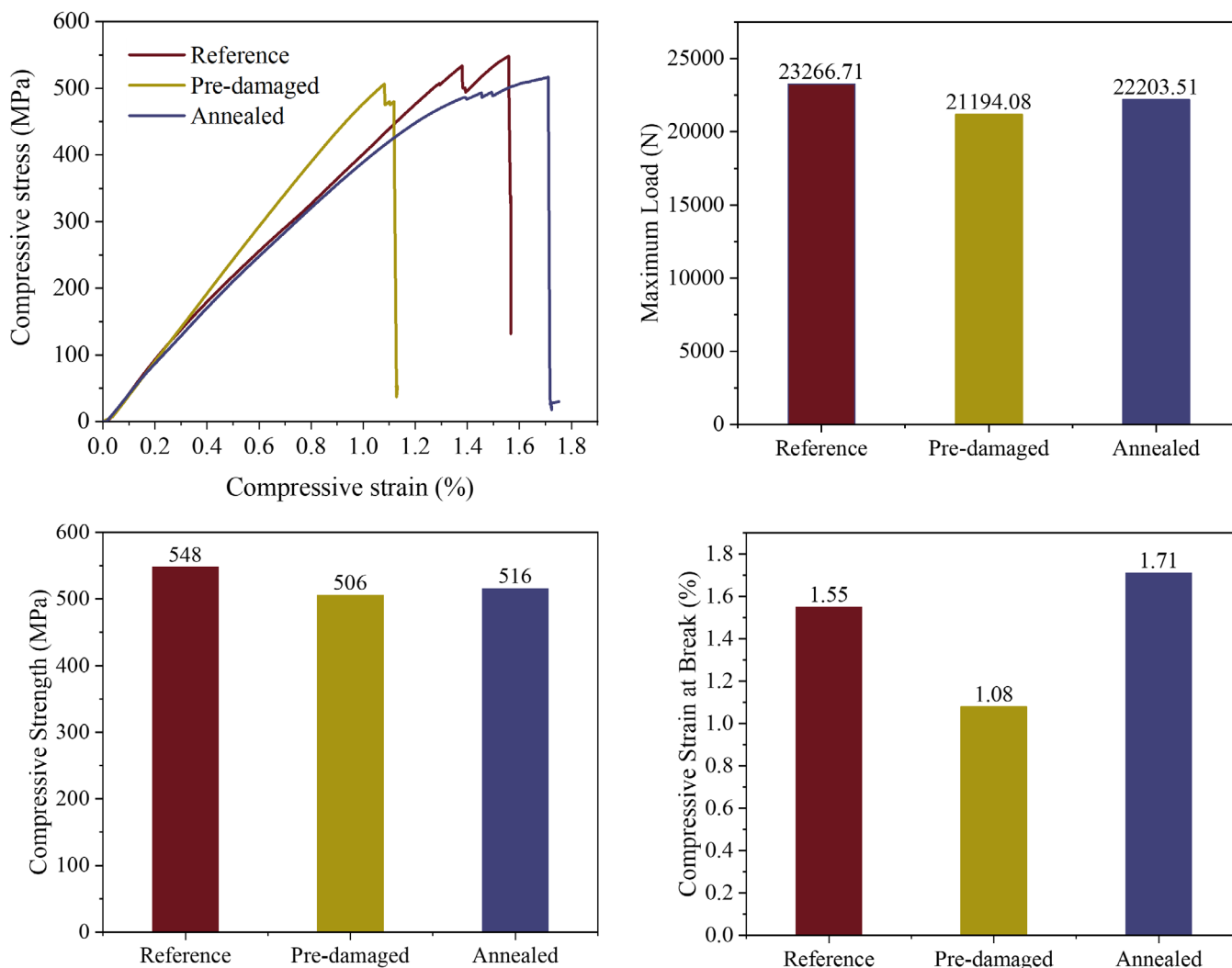


FIGURE 9 Compression test results for CF/PEKK samples with reference, pre-damaged, and annealed configurations with (A) representative compressive stress–strain curves and (B–D) bar charts for maximum load, compressive strength and compressive strain at break, respectively.

of 2.00% after annealing as presented in Figure 9C. The damage in the sample, especially in the PEKK matrix, acted as a stress concentrator, hindering the distribution of applied load during the test. As the pre-damage initiated some micro-cracks in the sample, the failure started at a lower stress level, contributing to the reduction in both maximum load capacity and compression strength.⁴² However, as the annealing redistributes internal stresses and induces stress relaxation, affects the overall mechanical and failure behavior. Furthermore, pre-damages significantly affected the compressive strain properties of the samples as seen in the bar chart in Figure 9D. The compressive strain at the point of failure in the pre-damaged sample decreased from 1.55% to 1.08%. This reduction indicates increased brittleness of the thermoplastic matrix.

The matrix material plays a crucial role in providing lateral stability to the fibers, preventing or delaying

failure under compressive load. Therefore, it is crucial to understand the compressive properties of thermoplastic composites for designing and utilizing in structural applications. In order to better understand the behavior of the CF/PEKK samples under compressive load, all experiments are supported by the AE inspection. The cluster ranges obtained from acoustic emission inspection that represent the damage types for the compression samples are given in Figure 10, where the cluster ranges slightly vary under compressive load. The optimal number of clusters is identified as three for the compression test: the first cluster in the 0–190 kHz frequency range, corresponds to matrix cracking,⁴⁵ the second cluster in the, 140–580 kHz, is associated with the fiber/matrix interface failure, as defined previously in the literature,⁴⁶ and consequently, the third cluster in the frequency in the 500–650 kHz range corresponds to fiber-related failure.⁴⁷

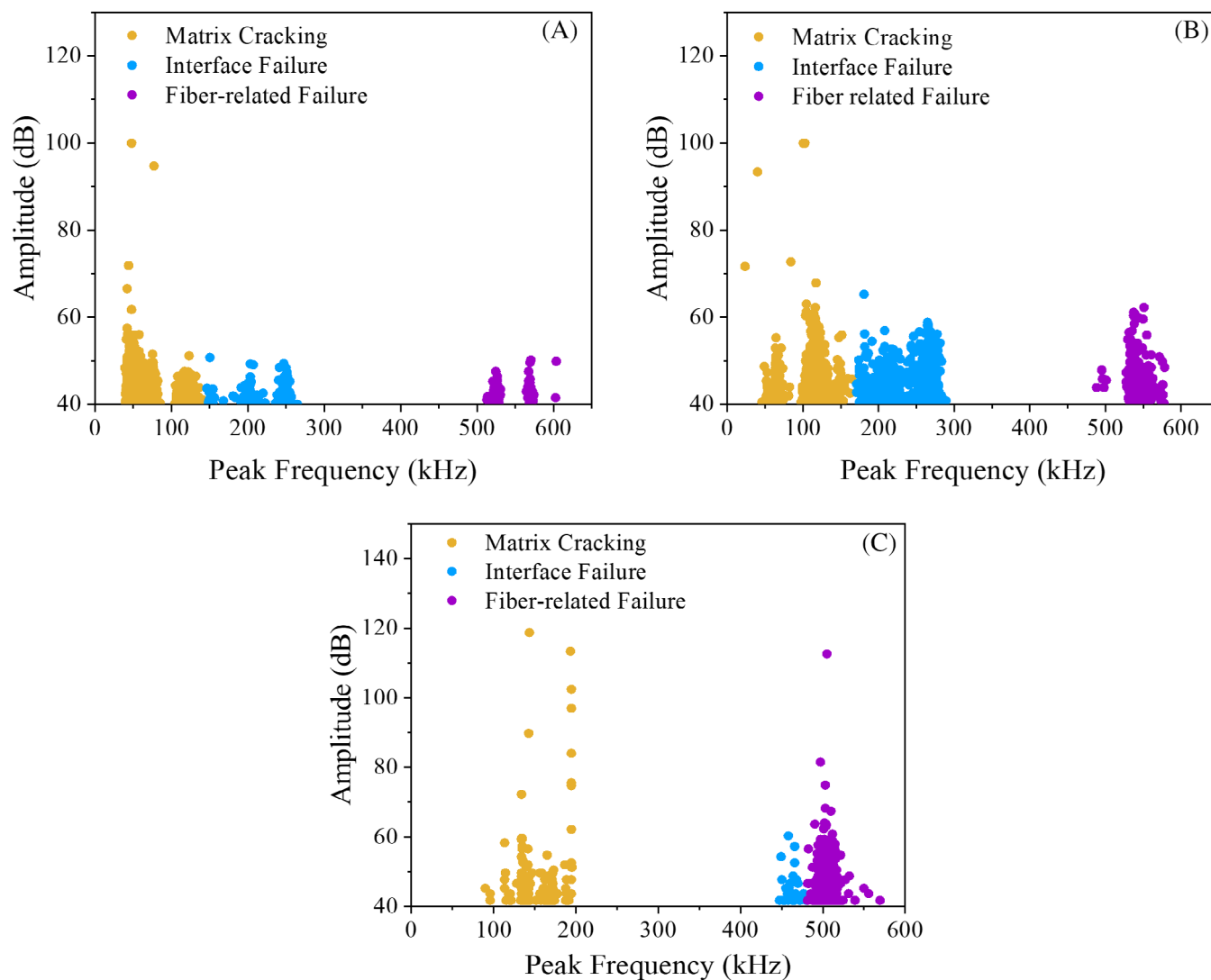


FIGURE 10 Clustered AE results of compression test for each damage type with peak amplitude and peak frequency graphs for (A) reference, (B) pre-damaged, (C) annealed CF/PEKK composite samples.

AE results provide insights into the failure modes for each sample. The AE analysis results and stress-strain graphs for reference, pre-damaged, and annealed compression samples are given in Figure 11. The CF/PEKK samples show a matrix dominant failure with a 92% percentage of matrix cracking cumulative counts under compressive load (Figure 11A). The composite likely exhibits a brittle response with the matrix playing a crucial role in load bearing. Hence, under compressive loading, the performance is highly influenced by the PEKK matrix. Cumulative counts of matrix cracking and interface failures raised in the elastic region. Subsequently, fiber-related failure causes a drop in strength at a strain level of 1.41%. Therefore, the initial drop in stress can be attributed to fiber-related failure. However, strength recovered due to the inner symmetrical layers in the composite until the

failure.⁴³ The sample lost its integrity by delamination of the inner layer and subsequently failed. Sitohang et al.⁴⁸ mentioned that 0° plies carry most of the load under compression and failure occurred when the fracture of the outer 0° ply in the gauge section. Transverse cracks and matrix cracking are observed near the edges of the sample, as shown in the optical microscopy images in Figure 12A. The progressive growth of cracks and especially buckling of the outer layers cause splaying of the other layers and finally delamination.

In the pre-damaged sample, the compression test is completed in a short period and cumulative count signals of each damage type started earlier compared to the reference sample (Figure 11B), with matrix cracking being the dominant failure type similar to the reference sample. However, the change in the percentage distribution of

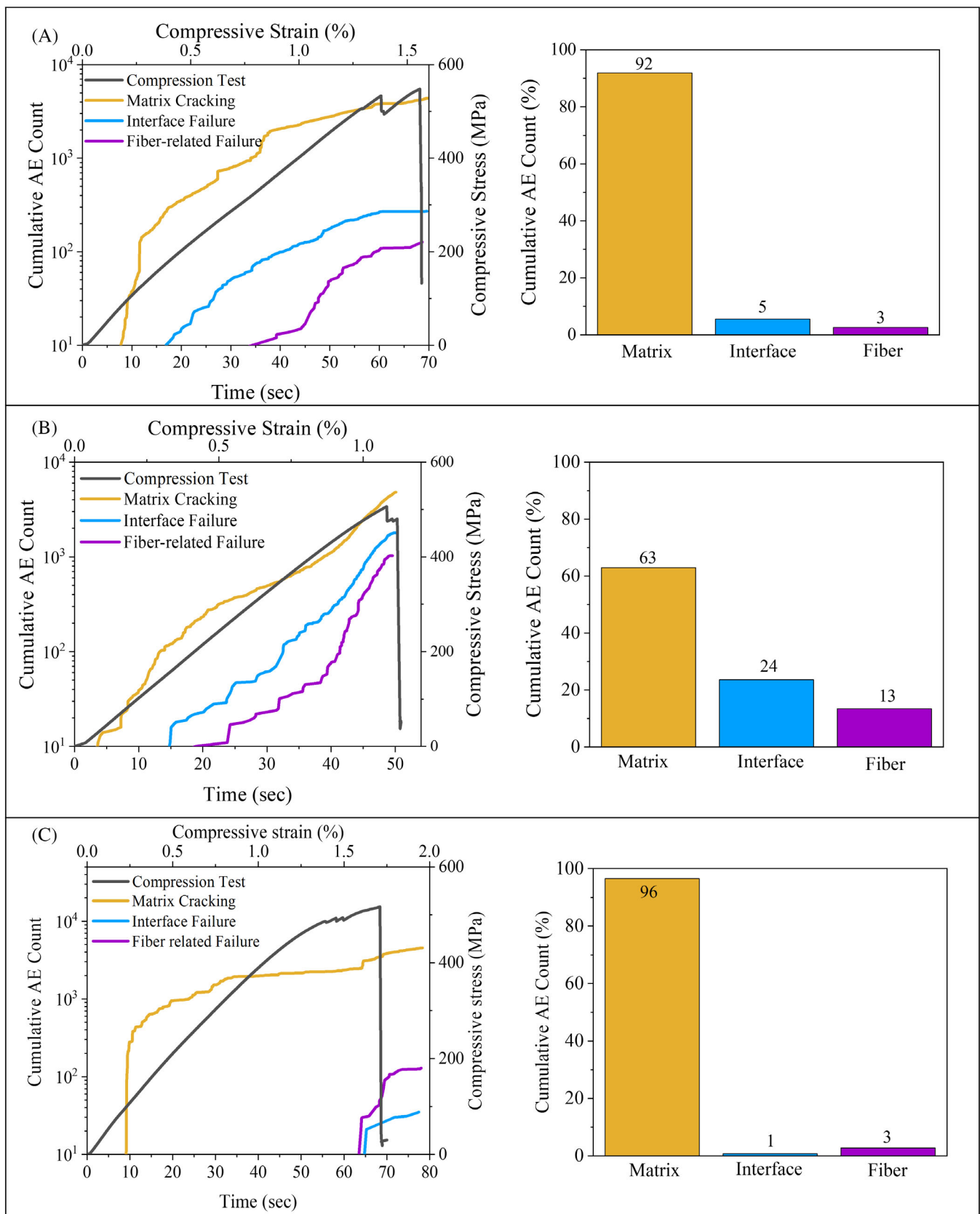


FIGURE 11 Cumulative AE count curves with compression stress–strain curve alongside percentage failure type distributions (fiber-related, matrix cracking, interface failure) for (A) reference, (B) pre-damaged, (C) annealed CF/PEKK composite samples (The AE counts correlate failure mechanisms with stress–strain behavior under compressive load, showing the percentage distribution of each failure type at maximum strain).

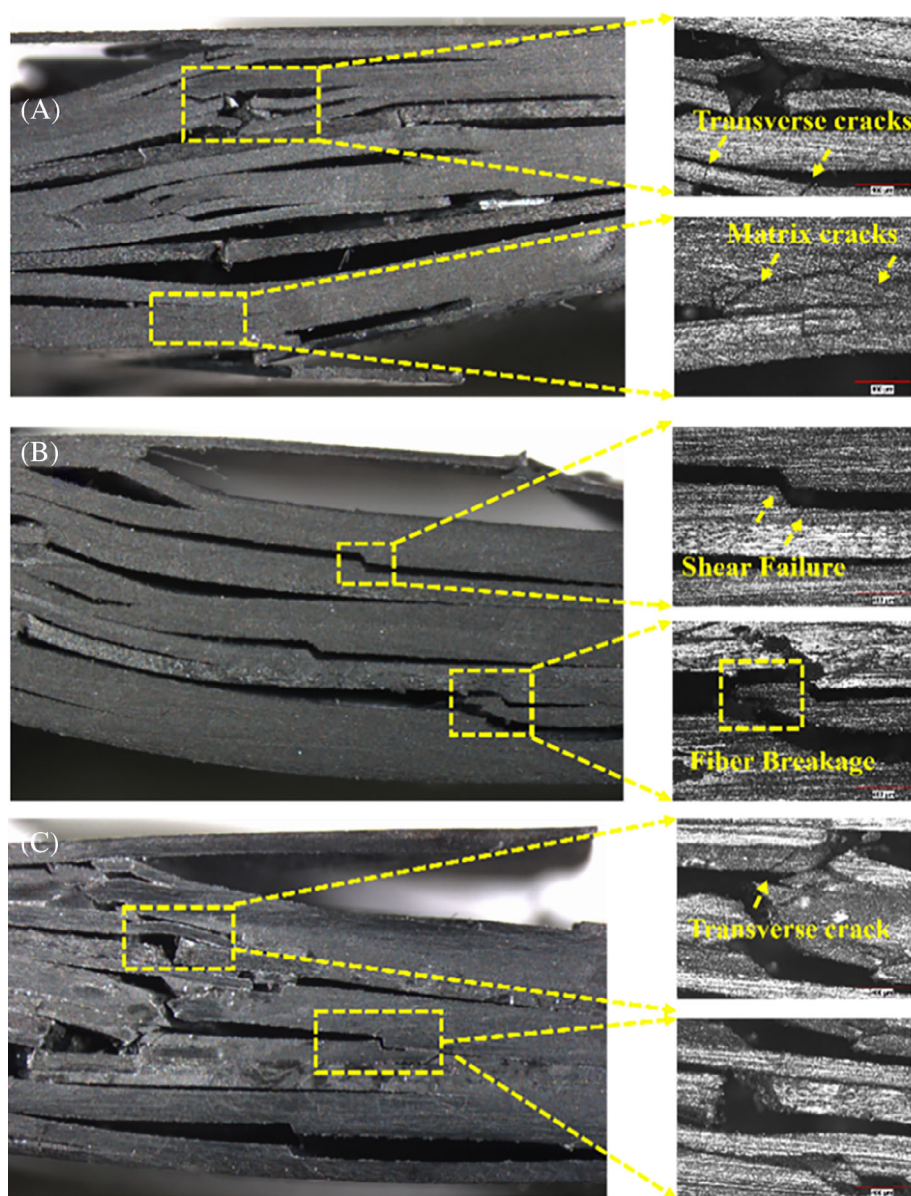


FIGURE 12 Optical microscopy images after compression test; (A) reference, (B) pre-damaged, (C) annealed CF/PEKK composite samples.

failure types reflects different damage mechanisms in pre-damaged samples. The applied pre-load results in the formation of micro-cracks in the PEKK matrix, leading to a decrease in the percentage of cumulative counts related to matrix cracking. Nevertheless, the presence of pre-damages leads to an increased percentage of interface and fiber-related failures, from 5% to 24%, and from 3% to 13%, respectively. Additionally, the thermoplastic matrix displays increased brittleness due to pre-damage formation as a consequence of the applied pre-load. These pre-damages have the potential to initiate rapid crack propagation in the matrix and at the interface, leading to fiber breakage. Consequently, a more brittle failure is observed compared to the reference sample.⁴⁹ The one-stage failure in the compression graph can be attributed to the brittle fracture of the sample since the merged

damages caused the failure of the matrix, interface, and fiber breakage step by step. Moreover, as the micro-cracks act as stress concentrators, stress is transferred from the intact regions to the areas surrounding the micro-cracks and leads to an increase in modulus as seen compressive stress-strain curve of the pre-damaged sample in Figure 9A.^{50,51} This shift in the damage mechanism, observed as a through-thickness shear failure, is evident in the optical microscopy images in Figure 12B. There is no transverse matrix cracking observed in the optical microscopy images, indicating a decrease in cumulative counts of matrix cracking-related failures. The coalescence of micro-cracks propagates the damage across the entire sample, ultimately leading to sample failure due to loss of structural integrity, as described in the study by Opelt et al.⁴³

On the other hand, the annealed sample continues to exhibit a high percentage of matrix-related failure with a cumulative count of 96% (Figure 11C). It is evident that the damage behavior is more similar to the reference sample including the test time. As the compressive load continues to increase, interface failure initiates, ultimately leading to the loss of sample integrity and fracture. Additionally, the increased matrix contribution suggests that annealing further strengthened the matrix, resulting resilient composite under compressive loading. The low incidence of interface failure suggests improved bonding between the fibers and the matrix. This improvement ultimately increases the compression strength of the sample as the compressive strength of the annealed sample increased to 516 MPa from 506 MPa compared to the pre-damaged sample. Moreover, the failure similarities between the reference and the annealed sample are seen in the microscopy images of fracture surfaces as given in Figure 12A,C, respectively. The annealing process results in the closure of micro-damages in the material (Figure 12C), leading to fracture behavior similar to that of the reference sample under the compression load, and reduced delamination propagation compared to the pre-damaged sample. That is particularly evident in the annealed samples, which exhibited higher compression strength.

The findings of mechanical analysis indicate that the annealing process has the potential to heal cracks in the composite and enhance its final failure behavior. Chanteli et al.⁵² demonstrated that annealing CF/PEEK samples after the automated tape-laying process altered the failure behavior in interlaminar shear strength and open hole compression analyses. The samples exhibited negligible delamination and crack formation. The controlled heating and cooling process of annealing helps gain mobility and molecular reorganization, relieving the internal stresses. As a result, any existing micro-cracks in the matrix could be filled up or become less pronounced.

4 | CONCLUSION

This study aims to investigate the impact of annealing on pre-existing damages and to highlight the mechanical and fracture behavior of CF/PEKK composites produced through the VBO process. It addresses a critical gap in the literature regarding the lack of research on the effect of annealing treatment on recovering damages in thermoplastic composites. The void content analysis reveals a well-consolidated composite with void content comparable to aerospace-grade quality, consistent with findings from previous studies using the same manufacturing method. The thermal characteristics show that annealing above the glass transition temperature induces partial melting and

recrystallization, resulting in increased T_g and crystallinity, thereby improving mechanical properties.

Three point bending and compression tests, assisted by acoustic emission (AE) inspection, provide valuable insights into the pre-existing damages and the subsequent effects of annealing. The changes observed in the cumulative acoustic counts reflect the impact of pre-existing damages and the annealing process on the mechanical behavior of composites, with implications for their strength and overall performance. In three-point bending tests, which induce flexural stresses, fiber-related failures are dominant. Conversely, matrix-related failures are dominant under compressive load. The presence of pre-existing damages introduces additional complexities in both tests, leading to increased contributions from matrix and interface failures. The differences in mechanical behavior and AE inspection between three point bending and compression tests can be attributed to the unique stress states and loading conditions in each test, as well as the specific characteristics introduced by the pre-existing damages and the effects of the annealing process. The changes in failure percentages reflect the diverse failure mechanisms operating under different loading conditions.

In summary, the annealing process effectively leads to enhanced structural integrity. The findings suggest that annealing has the potential to enhance the mechanical properties and failure behavior of thermoplastic composite laminates, offering valuable insights for the development and application of repair methods in aerospace and other industries. Further, varying annealing conditions, alongside alternative NDE techniques investigation will provide a deeper understanding of thermal treatment effects on thermoplastic composites. This approach will enhance the practical relevance of the findings and facilitate the development of more effective repair strategies for a wider range of thermoplastic composite structures.

ACKNOWLEDGMENTS

This study was supported by Scientific and Technological Research Council of Turkey (TUBITAK) under the Grant Numbers 221M565 and 218M709. The authors thank TUBITAK for their supports.

DATA AVAILABILITY STATEMENT

Data will be made available on request.

ORCID

Sinem Elmas  <https://orcid.org/0000-0002-9745-9680>

Mehmet Yildiz  <https://orcid.org/0000-0003-1626-5858>

Hatice S. Sas  <https://orcid.org/0000-0002-5179-2509>

REFERENCES

1. Amedewovo L, Levy A, de Parscau du Plessix B, Orgéas L, Le Corre S. Online characterization of moisture transport in a

- high-performance carbon fiber-reinforced thermoplastic composite at high temperatures: Identification of diffusion kinetics. *Compos Part B Eng.* 2023;256:110629.
2. Amedewovo L, Levy A, de Parscau du Plessix B, et al. A methodology for online characterization of the deconsolidation of fiber-reinforced thermoplastic composite laminates. *Compos Part A Appl Sci Manuf.* 2023;167:107412.
 3. Swamy JN, Grouve WJB, Wijskamp S, Akkerman R. An experimental study on the role of different void removal mechanisms in VBO processing of advanced thermoplastic composites. *J Reinf Plast Compos.* 2024;43(3-4):183-194. doi:10.1177/07316844231159134
 4. Mazur RL, Cândido GM, Rezende MC, Botelho EC. Accelerated aging effects on carbon fiber PEKK composites manufactured by hot compression molding. *J Thermoplast Compos Mater.* 2016;29:1429-1442.
 5. Centea T, Grunenfelder LK, Nutt SR. A review of out-of-autoclave prepregs – material properties, process phenomena, and manufacturing considerations. *Compos Part A Appl Sci Manuf.* 2015;70:132-154.
 6. Zhang D, Heider D, Gillespie JW. Void reduction of high-performance thermoplastic composites via oven vacuum bag processing. *J Compos Mater.* 2017;51:4219-4230.
 7. Barroeta Robles J, Dubé M, Hubert P, Yousefpour A. Repair of thermoplastic composites: An overview. *Adv Manuf Polym Compos Sci.* 2022;8:68.
 8. Sukur EF, Elmas S, Seyyednourani M, Eskizeybek V, Yildiz M, Sas HS. Effects of meso- and micro-scale defects on hygrothermal aging behavior of glass fiber reinforced composites. *Polym Compos.* 2022;43:8396-8408.
 9. Akgun S, Senol CO, Kilic G, Tabrizi IE, Yildiz M. A novel damage evaluation of CFRPs under mode-I loading by using multi-instrument structural health monitoring methods. *Eng Fract Mech.* 2023;286:109291.
 10. Yildirim C, Tabrizi IE, Al-Nadhari A, Topal S, Beylergil B, Yildiz M. Characterizing damage evolution of CF/PEKK composites under tensile loading through multi-instrument structural health monitoring techniques. *Compos Part A Appl Sci Manuf.* 2023;175:107817.
 11. Sukur EF, Elmas S, Seyyednourani M, Eskizeybek V, Yildiz M, Sas HS. A rational study on the hydrothermal aging of AFP manufactured CF/polyetherketoneketone composites with in-situ consolidation supported by acoustic emission inspection. *J Appl Polym Sci.* 2022;139:1.
 12. Li W, Palardy G. Investigation of welding repair methods for thermoplastic composite joints. *Compos Part B Eng.* 2023; 264:264.
 13. Ahmadi F. Study of process-induced stresses and deformations in thermoplastic matrix composites. 2023.
 14. Regis M, Bellare A, Pascolini T, Bracco P. Characterization of thermally annealed PEEK and CFR-PEEK composites: structure-properties relationships. *Polym Degrad Stab.* 2017;136:121-130.
 15. Yu W, Wang X, Yin X, Ferraris E, Zhang J. The effects of thermal annealing on the performance of material extrusion 3D printed polymer parts. *Mater Des.* 2023;226:111687.
 16. Conejo L d S, Santos LF d P, Ribeiro B, et al. Reconsolidation effect on impact, compression after impact and thermal properties of poly (aryl ether ketone) composites for aeronautical applications. *J Thermoplast Compos Mater.* 2023;36:2562.
 17. Toray Cetex® TC1320 - Toray Advanced Composites. <https://www.toraytac.com/product-explorer/products/yljT/Toray-Cetex-TC1320> (accessed January 24, 2024)
 18. Karimi S, Louyeh PY, Barzegar A, Yildiz M, Sas HS. A study of post-processing for AFP-fabricated thermoplastic composites with void content and air permeability characterization. *J Reinf Plast Compos.* 2023;43(9-10):490-503.
 19. Elkolali M, Nogueira LP, Rønning PO, Alcocer A. Void content determination of carbon fiber reinforced polymers: A comparison between destructive and non-destructive methods. *Polymer.* 2022;14:1212.
 20. Quiroga Cortés L, Caussé N, Dantras E, Lonjon A, Lacabanne C. Morphology and dynamical mechanical properties of poly ether ketone ketone (PEKK) with meta phenyl links. *J Appl Polym Sci.* 2016;133:1-10.
 21. Pariyski S. Technische Universität München. 2022.
 22. Caliński T, Harabasz J. A dendrite method for cluster analysis. *Commun Stat.* 1974;3:1-27.
 23. Gul S, Tabrizi IE, Okan BS, Kefal A, Yildiz M. An experimental investigation on damage mechanisms of thick hybrid composite structures under flexural loading using multi-instrument measurements. *Aerosp Sci Technol.* 2021;117:117.
 24. Parlevliet PP, Bersee HEN, Beukers A. Residual stresses in thermoplastic composites - A study of the literature - Part I: Formation of residual stresses. *Compos Part A Appl Sci Manuf.* 2006;37(11):1847-1857.
 25. Meng Q, Gu Y, Luo L, Wang S, Li M, Zhang Z. Annealing effect on crystalline structure and mechanical properties in long glass fiber reinforced polyamide 66. *J Appl Polym Sci.* 2017;134:1.
 26. Zhang J, Liu G, An P, et al. The effect of cooling rates on crystallization and low-velocity impact behaviour of carbon fibre reinforced poly(aryl ether ketone) composites. *Compos Part B Eng.* 2023;254:254.
 27. Wang W, Zhao G, Wu X, Zhai Z. The effect of high temperature annealing process on crystallization process of polypropylene, mechanical properties, and surface quality of plastic parts. *J Appl Polym Sci.* 2015;132:132.
 28. Hoang V-T, Kwon B-S, Sung J-W, et al. Postprocessing method-induced mechanical properties of carbon fiber-reinforced thermoplastic composites. *J Thermoplast Compos Mater.* 2020; 36(1):432-447.
 29. Cho BG, Ram Joshi S, Hun Han J, Kim GH, Bin Park Y. Interphase strengthening of carbon fiber/polyamide 6 composites through mixture of sizing agent and reduced graphene oxide coating. *Compos Part A Appl Sci Manuf.* 2021;149:106521.
 30. Ostberg GMK, Seferis JC. Annealing effects on the crystallinity of polyetheretherketone (PEEK) and its carbon fiber composite. *J Appl Polym Sci.* 1987;33:29-39.
 31. Wang J, Yan F, Liu H, Jiang P. Research on preparation of phosphate-modified animal glue binder for foundry use. *R Soc Open Sci.* 2018;5:5.
 32. Yu X, Song W, Zheng J, et al. Effects of low-pressure annealing on the performance of 3D printed CF/PEEK composites. *Chin J Mech Eng Addit Manuf Front.* 2023;2:100076.
 33. Ogunleye RO, Rusnakova S, Zaludek M, Emebu S. The influence of ply stacking sequence on mechanical properties of carbon/epoxy composite laminates. *Polymers (Basel).* 2022;14:14.
 34. Qin R, Zhou W, Han KN, Zhang YJ, Ma LH. Comparison on mechanical properties, damage evolution and aging effects of

- multi-delaminated composites under three point bending. *SN Appl Sci*. 2020;2:2.
35. Uematsu H, Mune K, Nishimura S, et al. Fracture properties of quasi-isotropic carbon-fiber-reinforced polyamide 6 laminates with different crystal structure of polyamide 6 due to surface profiles of carbon fibers. *Compos Part A Appl Sci Manuf*. 2022;154:154.
 36. Lv X, Yang S, Pei X, Zhang Y, Wang Q, Wang T. Enhanced mechanical and tribological properties of 3D printed short carbon fiber reinforced polyether ether ketone composites. *Polym Compos*. 2024;45.
 37. Zhao J, Guo C, Zuo X, et al. Effective mechanical properties of injection-molded short fiber reinforced PEEK composites using periodic homogenization. *Adv Compos Hybrid Mater*. 2022;5: 2964-2976.
 38. Yilmaz C, Yildiz M. A study on correlating reduction in Poisson's ratio with transverse crack and delamination through acoustic emission signals. *Polym Test*. 2017;63:47-53.
 39. AlKhateab B, Tabrizi IE, Zanjani JSM, et al. Damage mechanisms in CFRP/HNT laminates under flexural and in-plane shear loadings using experimental and numerical methods. *Compos Part A Appl Sci Manuf*. 2020;136:136.
 40. De Groot PJ, Wijnen PAM, Janssen RBF. Real-time frequency determination of acoustic emission for different fracture mechanisms in carbon/epoxy composites. 1995;55:405-412.
 41. Khan RMA, Tabrizi IE, Ali HQ, Demir E, Yildiz M. Investigation on interlaminar delamination tendency of multidirectional carbon fiber composites. *Polym Test*. 2020;90:90.
 42. McElroy M, Jackson W, Olsson R, Hellström P, Tsampas S, Pankow M. Interaction of delaminations and matrix cracks in a CFRP plate, part I: a test method for model validation. *Compos Part A Appl Sci Manuf*. 2017;103:314-326.
 43. Opelt CV, Cândido GM, Rezende MC. Compressive failure of fiber reinforced polymer composites: a fractographic study of the compression failure modes. *Mater Today Commun*. 2018;15:218-227.
 44. Liu A, Zou Y, Chen Y, Hu J, Wang B. Experimental investigation of impact resistance and compression behavior of CF/PEEK laminates after hot-press fusion repair with different stacking sequences. 2023;44:6467-6481.
 45. Santulli C. Matrix Cracking Detection by Acoustic Emission in Polymer Composites and Counts/Duration Ratio.
 46. Arumugam V, Sidharth AAP, Santulli C. Failure modes characterization of impacted carbon fibre reinforced plastics laminates under compression loading using acoustic emission. *J Compos Mater*. 2014;48:3457-3468.
 47. Huguet S, Godin N, Gaertner R, Salmon L, Villard D. Use of acoustic emission to identify damage modes in glass fibre reinforced polyester.
 48. Sitohang RDR, Grouve WJB, Warnet LL, Akkerman R. Effect of in-plane fiber waviness defects on the compressive properties of quasi-isotropic thermoplastic composites. *Compos Struct*. 2021; 272:272.
 49. Abdel-magid B, Ziaee S, Gass K, Schneider M. The combined effects of load, moisture and temperature on the properties of E-glass/epoxy composites. 2005;71:320-326.
 50. Seyyednourani M, Akgun S, Ulus H, Yildiz M, Sas HS. Experimental investigation on compression-after-impact (CAI) response of aerospace grade thermoset composites under low-temperature conditions assisted with acoustic emission monitoring. *Compos Struct*. 2023;321:321.
 51. Yan M, Liu Y, Jiang W, et al. Mechanism of matrix influencing the cryogenic mechanical property of carbon fibre reinforced epoxy resin composite. *Compos Commun*. 2022;33:101220.
 52. Chanteli A, Bandaru AK, Peeters D, O'Higgins RM, Weaver PM. Influence of repress treatment on carbon fibre-reinforced PEEK composites manufactured using laser-assisted automatic tape placement. *Compos Struct*. 2020;248:112539.

SUPPORTING INFORMATION

Additional supporting information can be found online in the Supporting Information section at the end of this article.

How to cite this article: Elmas S, Atac B, Senol CO, Topal S, Yildiz M, Sas HS. Annealing impact on mechanical performance and failure analysis assisted with acoustic inspection of carbon fiber reinforced poly-ether-ketone-ketone composites under flexural and compressive loads. *Polym Compos*. 2024;1-19. doi:[10.1002/pc.29199](https://doi.org/10.1002/pc.29199)